Epitaxial Phase Transformation between Cylindrical and Double Gyroid Mesophases

Lei Zhu,[1] Lu Sun,[1] Jianjun Miao,[1] Li Cui,[1] Qing Ge,[2] Roderic P. Quirk,[2] Chenchen Xue,[2] Stephen Z. D. Cheng,[2] Benjamin S. Hsiao,[3] Carlos A. Avila-Orta,[3] Igors Sics,[3] and Marie E. Cantino[4]

[1]Polymer Program, Institute of Materials Science and Department of Chemical Engineering, University of Connecticut, Storrs, CT 06269-3136
[2]Maurice Morton Institute and Department of Polymer Science, University of Akron, Akron, OH 44325
[3]Chemistry Department, State University of New York at Stony Brook, Stony Brook, NY 11794
[4]Department of Physiology and Neurobiology, University of Connecticut, Storrs, CT 06269

ABSTRACT

Complex phase transformation between the hexagonal cylinder (Hex) and double gyroid (G) phases in a polystyrene-*block*-poly(ethylene oxide) **(**PS-*b*-PEO) diblock copolymer was investigated using two-dimensional (2D) synchrotron small-angle X-ray scattering (SAXS), and transmission electron microscope (TEM). The PS-*b*-PEO sample contained a small population of another bicontinuous cubic phase having an $Im\bar{3}m$ symmetry. These two bicontinuous cubic phases (G and $Im\bar{3}m$) had the same unit cell dimensions. Under a large-amplitude reciprocating shear, the bicontinuous cubic phases transformed into a "single-crystal"-like Hex phase. When annealed at 150 °C for 40 min, the Hex phase partially transformed into well-oriented twinned structures of the G and $Im\bar{3}m$ phases without significant loss of orientation in 2D SAXS measurements. Epitaxial phase transformation relationships between the Hex/G and Hex/ $Im\bar{3}m$ phases were identified. The mechanism of the Hex $\rightarrow$ G transformation was examined by TEM.

INTRODUCTION

Similar to amphiphilic surfactants and lipids, diblock copolymers are capable of self-organizing into long-range ordered mesophases on nanometer length scales [1], which makes them attractive in the development of nanotechnology and nanofabrication. [2] The phase transformations between the double gyroid (G) phase and neighboring phases have received extensive attention since Charvolin and co-workers [3,4] studied the epitaxial relationships in the transformations between the G $\leftrightarrow$ lamellar (L) and G $\leftrightarrow$ cylindrical (Hex) phases in nonionic surfactants. [5] In a G $\leftrightarrow$ L transformation, the $[100]_L$ became the $[121]_G$, and *vice versa*. In a G $\leftrightarrow$ Hex transformation, the $[100]_{Hex}$ transformed to the $[1\bar{2}1]_G$ and the cylinder axes $[001]_{Hex}$ became the $[111]_G$ direction, and *vice versa*. In the epitaxial phase transformations, the two phases matched not only in orientation, but in the periodicity as well, *e.g.*, the $d_{100,\,L} \approx d_{211,\,G}$ and $d_{100,\,Hex} \approx d_{211,\,G}$. Other than the G phase, a new bicontinuous cubic morphology was recently reported for block copolymer/organically modified ceramic (*ormercer*) nanocomposites, namely, the P phase or so-called "Plumber's Nightmare" [6] phase having an $Im\bar{3}m$ symmetry. [7-9]

In this work, we report our preliminary results on complex phase transformations between the Hex and bicontinuous cubic phases (*i.e.*, G and $Im\bar{3}m$ phases) in a polystyrene-*block*-

poly(ethylene oxide) (PS-*b*-PEO) diblock copolymer, using high-resolution synchrotron small angle X-ray scattering (SAXS). After the sample was cast from chloroform solution and annealed at 150 °C, a G phase was observed with a small "contamination" of $Im\bar{3}m$ phase. Under a large-amplitude reciprocating shear, the bicontinuous cubic phases were found to transform into a "single-crystal"-like Hex phase. Annealing the sample at elevated temperatures (> 140 °C), part of the oriented Hex phase could transform back into twinned bicontinuous cubic phases, having a majority of the G twins and a small fraction of twinned $Im\bar{3}m$ structures. The epitaxial relationships for both phase transitions were studied. A snapshot of Hex to G phase transformation was revealed in real space using transmission electron microscopy (TEM).

EXPERIMENTAL DETAILS

Materials. A PS-*b*-PEO diblock copolymer with M_n^{PEO} = 11.6k g/mol and M_n^{PS} = 18.5k g/mol was synthesized by anionic block copolymerization. [10] The PEO volume fraction in the melt is 0.374. The polydispersity was determined by size-exclusion chromatography (SEC) to be 1.09. The sample was cast from chloroform solution and annealed at 120 °C for 12 hrs to allow equilibrium microphase separation. The order-to-disorder transition temperature (T_{ODT}) was determined by both low-frequency rheometry and SAXS at *ca*. 210 °C. Differential scanning calorimetry (DSC) results show that the melting point of PEO crystals is ~51 °C. The microphase-separated sample was subjected to a planar reciprocating shear at 120 °C under a dry nitrogen atmosphere, using a laboratory-built shear apparatus. The shear frequency was around 0.5 Hz, and the amplitude was ~150 %. The shear direction was defined as the *x* direction, and the shear gradient was along the *y* direction. Sample size was around 1 mm × 1 mm × 0.2 mm.

Equipment and Experiments. Two-dimensional (2D) SAXS experiment was performed at the synchrotron X-ray beamline X27C at the National Synchrotron Light Source in Brookhaven National Laboratory. The wavelength of the X-ray beam was 0.137 nm. The beam center and scattering vector q ($q = 4\pi\sin\theta/\lambda$, where 2θ is the scattering angle and λ is the wavelength) were calibrated using silver behenate with the first order reflection peak at 1.076 nm^{-1}. TEM experiments were performed on a Philips EM300 at an accelerating voltage of 80 kV. Thin sections of *ca*. 75-100 nm thicknesses were obtained at -40 °C using a Leica Ultracut UCT microtome equipped with a diamond knife. The thin sections were collected onto 400 mesh TEM grids, and were stained in RuO_4 vapor at room temperature for 20 min. [11]

RESULTS AND DISCUSSION

Hex to G Phase Transformation Studied by 2D SAXS

When the PS-*b*-PEO sample was subjected to a large-amplitude planar shear, a "single-crystal"-like Hex phase was obtained. The 2D SAXS patterns with the X-ray along three orthogonal (*x*, *y*, and *z*) directions are shown in the top of Figure 1. The SAXS pattern along the *x*-direction shows clearly six-fold symmetry with *q*-ratios being 1 : √3 : √4 : √7 : √9. In the SAXS pattern along the *y*-direction, only the $(\bar{1}20)$ reflections in the *z*-direction can be observed [the weak and diffuse (100) reflections result from the slight misorientation of the hexagonal cylinders], while the (100), (200), and (300) reflections are seen in the *z*-direction. These results are evident for a "single-crystal"-like Hex phase obtained by a large amplitude

reciprocating shear, and the *x*, *y*, and *z*-directions correspond to the [001], [100], and [$\bar{1}$20] directions of the Hex structure, respectively.

The Hex to G phase transformation was carried out by isothermal annealing of the PS-*b*-PEO diblock copolymer at 150 °C for 40 min and then quenching to room temperature. The 2D SAXS patterns along the *x*, *y*, and *z* directions and the corresponding interpretations are shown in the bottom of Figure 1. As the X-ray beam is along the *x*-direction, one can see that the Hex phase is transforming to the G phase, but has not yet completed as evidenced from the remaining Hex reflections. Our results show that annealing at higher temperatures and for longer times will lose microdomain orientation. From the 2D SAXS patterns along the *x*-direction for Hex and G phases, the epitaxial relationship clearly indicates that the Hex[001] corresponds to the G[111]. Some desmeared reflections are also observed, such as those weak reflections in the G(211) reflection ring, due to the misorientation of microdomains. From the 2D SAXS patterns along the *y*-direction for the Hex and G phases, the G ($20\bar{2}$) reflection is in the same direction as the Hex ($\bar{1}20$) reflection, confirming the Hex[$\bar{1}20$] $\rightarrow$ G[$20\bar{2}$] epitaxial relationship. The inner (121) reflection ring is observed due to mis-orientation of the microdomains, which otherwise should not exist in this pattern. The 2D SAXS pattern along the *z*-direction for the G phase is interpreted as twinned G[$20\bar{2}$] pattern. The twin element is the G(111) plane. Therefore, it also indicates an epitaxial relationship of Hex[100] $\rightarrow$ G[$1\bar{2}1$].

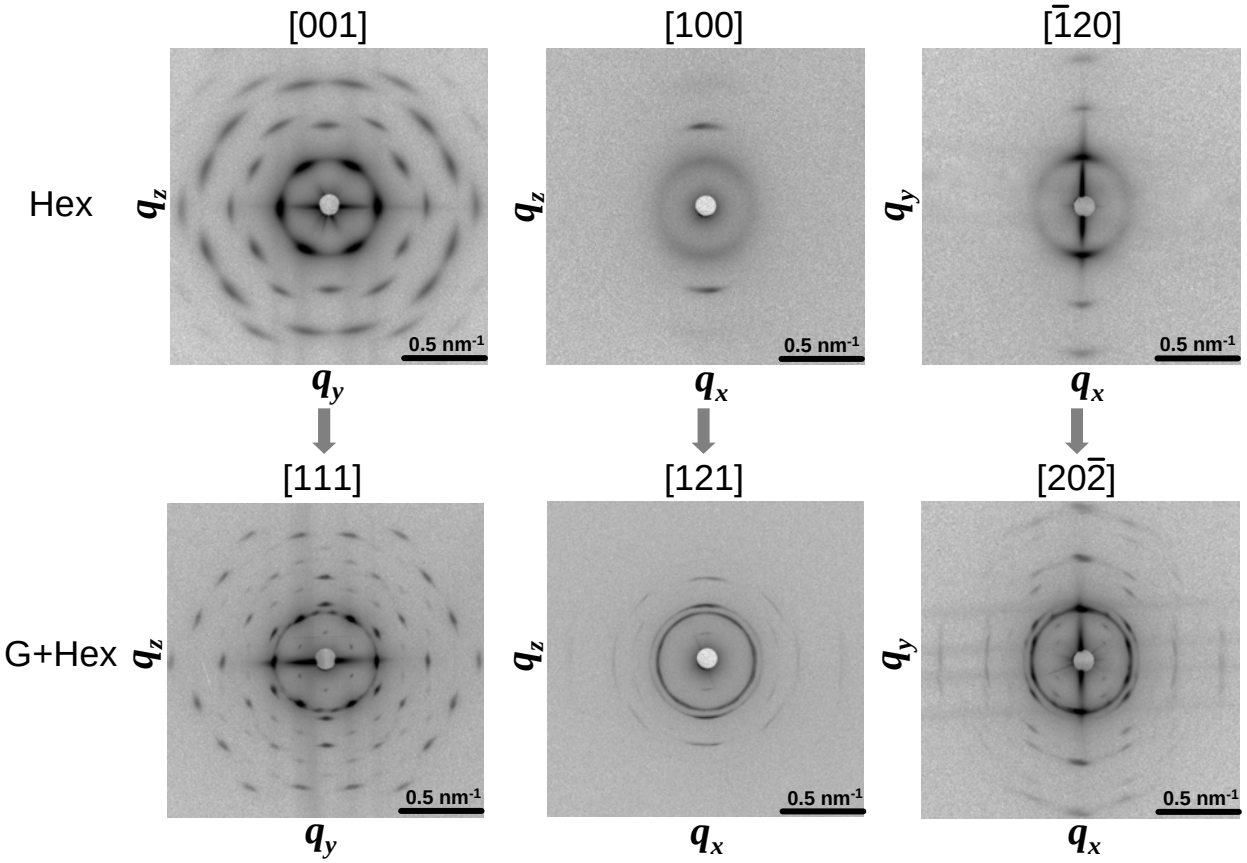

Figure 1. 2D SAXS patterns during epitaxial phase transformation from the Hex to the G. The 1st, 2nd, and 3rd columns correspond to the patterns as the X-ray beam is along the *x*, *y*, and *z* directions, respectively.

Visualization of the Hex to G Phase Transition

The incomplete phase transformation from Hex to G provides us an opportunity to study the transformation mechanism in diblock copolymers. The phase transformation along the G[111] (*i.e.*, Hex[001]) direction is seen in the bright-field TEM micrograph in Figure 2A. As one can see, the Hex phase directly transforms into the G phase with a well-defined epitaxial relationship (see the bottom of Figure 2A). The Hex[100] is exactly in the same direction as the G[211], and the *d*-spacing of Hex(100) is almost the same as the G(211) (21.0 nm *vs*. 20.0 nm). The Hex to G phase transition has been studied using self-consistent field theory, [12] and the results for χN = 17 and f = 0.35 are summarized in Figure 2B. The transition path is parameterized as s, where $d\,s^2 = \sum_i \delta\Phi_i^2$ ($\delta\Phi_i$ is the difference in the A- and B-segment densities), and the peak in the energy barrier defines s = 0. The two images on the left show top and side views of the Hex phase (s = -0.404). The cylinder at the center is among the 1/3 that develops a series of subtle bulges along the length. Three of its neighbors evolve into left-handed helices while the other three form right-handed helices. At s = -0.065, each bulge transforms into a five-fold coordinated junction by developing connections with the neighboring helices of a particular handedness, which alternates between adjacent bulges. At s = 0.230, the five-fold junctions break apart leaving a series of three-fold junctions characteristic of the G phase. Finally, the structure smoothly evolves into the G phase with s = 0.459. The TEM micrograph in Figure 2A shows preliminary evidence for this phase transformation mechanism. As indicated by arrow I, a three-fold connection between the cylinders is observed, which may represent the [001]-projection of a five-fold junction [three-dimensional (3D) schematics *b* or *c* in Figure 2B] and further develop into either a right- or a left-handed helix. The arrow II shows a six-fold connection between the cylinders, which is the [001]-projection of the 3D schematics *d* or *e* in Figure 2B. Here, the two free ends of the cylinders (3D schematic *c*) are highly unfavorable and should quickly form two four-fold junctions (3D schematic *d*) that would each break off to produce a three-fold junction. As seen in Figure 2A, the phase transition zone (or grain boundary) is indeed quite thin, which only involve less than one unit cell, as predicted in the

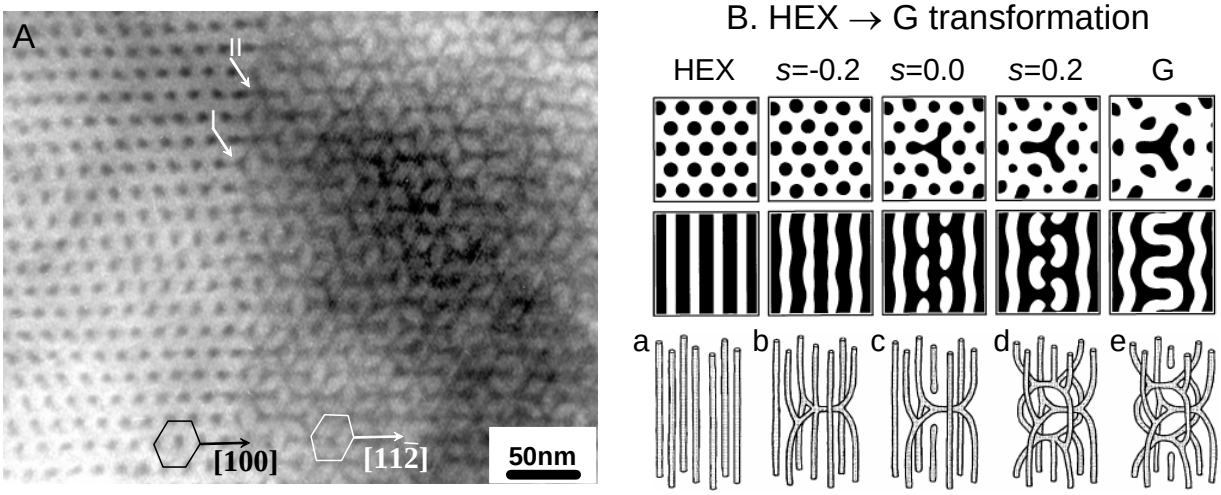

Figure 2. (A) TEM observation of epitaxial phase transition from the Hex to the G, and (B) schematic phase transformation mechanism predicted by Matsen, reprinted with permission from Ref. [12].

literature. [12] However, additional TEM observations along either $[100]_{Hex}$ or $[\bar{1}20]_{Hex}$ are desirable to unambiguously determine this phase transformation mechanism, and this work is still underway.

Determination of the $Im\bar{3}m$ Phase using 2D SAXS.

If one carefully examine the 2D SAXS patterns in the bottom of Figure 1, weak but clear and well-oriented reflections inside the G(211) reflection ring could be identified as another minority phase in the PS-*b*-PEO sample, since these reflections are forbidden by the $Ia\bar{3}d$ symmetry. They have a *q*-relationship of $\sqrt{2} : \sqrt{4}$ with respect to the rest of the G phase reflections. We tentatively determine this bicontinuous cubic phase to be an $Im\bar{3}m$ symmetry. The possibility of body-centered cubic (Bcc) spheres can be eliminated, since the PEO volume fraction is 0.37 and we also did not see Bcc morphology in our TEM experiments. The assignment of these reflections is shown in Figure 3. The calculated $Im\bar{3}m$ phase patterns fit well with the experimental results. Again, after phase transformation from the Hex phase, the $Im\bar{3}m$ phase is twinned as evidenced from the pattern along the *z* ($[10\bar{1}]$) direction in Figure 3C. It is clear that as the "single-crystal"-like Hex phase transforms to the $Im\bar{3}m$ phase, there are also following epitaxy relationships: Hex[001] $\rightarrow$ $Im\bar{3}m$ [222], Hex[100] $\rightarrow$ $Im\bar{3}m$ $[1\bar{2}1]$, and Hex$[\bar{1}20]$ $\rightarrow$ $Im\bar{3}m$ $[10\bar{1}]$. We can also see that the G phase has exactly the same orientation and *d*-spacing as the $Im\bar{3}m$ phase, since their major peaks superpose. To explicitly determine the morphology of this $Im\bar{3}m$ phase, detailed real space morphology and structure will be further studied by TEM experiments. This is also currently under investigation.

CONCLUSIONS

Complex epitaxial phase transitions between bicontinuous cubic and Hex phases in a PS-*b*-PEO diblock copolymer have been investigated. The sample has a typical G phase,

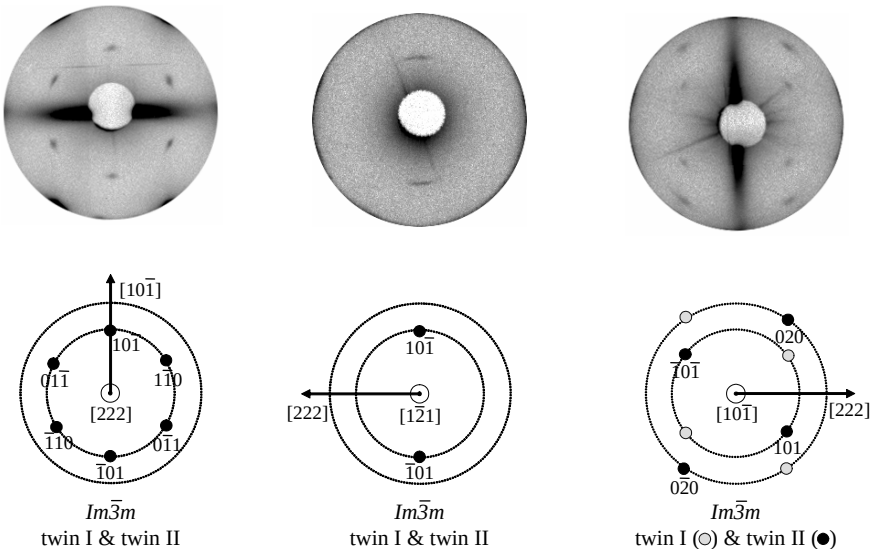

Figure 3. Interpretation of the 2D SAXS pattern along the [222], $[1\bar{2}1]$, and $[10\bar{1}]$ directions of the $Im\bar{3}m$ phase.

together with a small fraction of the $Im\bar{3}m$ phase. Like the cases in lyotropic liquid crystals, both bicontinuous cubic phases have the same unit cell dimensions. After a large-amplitude mechanical shear at 120 °C, the bicontinuous cubic sample exhibits a well-oriented Hex phase. Annealing this sample at 150 °C for 40 min, the Hex phase partially transforms into twinned G and $Im\bar{3}m$ phases with preserved orientations, as evidenced by 2D SAXS patterns. Epitaxial phase transformation relationships between the Hex/G and Hex/ $Im\bar{3}m$ phases are identified:

(1) Hex[001] $\rightarrow$ G[111], Hex[100] $\rightarrow$ G[$1\bar{2}1$], and Hex[$\bar{1}20$] $\rightarrow$ G[$20\bar{2}$];

(2) Hex[001] $\rightarrow$ $Im\bar{3}m$ [222], Hex[100] $\rightarrow$ $Im\bar{3}m$ [$1\bar{2}1$], and Hex[$\bar{1}20$] $\rightarrow$ $Im\bar{3}m$ [$10\bar{1}$].

The mechanism of the Hex $\rightarrow$ G transformation observed by TEM is consistent with previous theoretical prediction. [12]

ACKNOWLEDGEMENTS

This work was supported by the startup funds (University of Connecticut), University of Connecticut Research Foundation, NSF CAREER award (DMR-0348724), and 3M nontenured faculty award. The synchrotron SAXS experiments were carried out in the National Synchrotron Light Source, Brookhaven National Laboratory, supported by the Department of Energy (DE-FG02-99ER 45760).

REFERENCES

1. M. Muthukumar, C. K. Ober, E. L. Thomas, *Science* **277**, 1225 (1997).
2. C. Park, J. Yoon, E. L. Thomas, *Polymer* **44**, 6725 (2003).
3. Y. Rançon, J. Charvolin, *J. Phys. Chem.* **92**, 2646 (1988).
4. Y. Rançon, J. Charvolin, *J. Phys. Chem.* **92**, 6339 (1988).
5. M. Clerc, P. Laggner, A.-M. Levelut, G. Rapp, *J. Phys. II France* **5**, 901 (1995).
6. D. A. Huse, S. Leibler, *J. Phys.-Paris* **49**, 605 (1988).
7. A. C. Finnefrock, R. Ulrich, A. Du Chesne, C. C. Honeker, K. Schumacher, K. K. Unger, S. M. Gruner, U. Wiesner, *Angew. Chem. Int. Ed.* **40**, 1207 (2001).
8. P. F. W. Simon, R. Ulrich, H. W. Spiess, U. Wiesner, *Chem. Mater.* **13**, 3464 (2001).
9. Finnefrock, A. C. Ulrich, R. Toombes, G. E. S. Gruner, S. M. Wiesner, U. *J. Am. Chem. Soc.* **125**, 13084 (2003).
10. L. Zhu, S. Z. D. Cheng, B. H. Calhoun, Q. Ge, R. P. Quirk, E. L. Thomas, B. S. Hsiao, F. Yeh, B. Lotz, *Polymer* **42**, 5829 (2001).
11. Trent, J. S.; Scheinbeim, J. I.; Couchman, P. R. *Macromolecules* **16**, 589 (1983).
12. M. W. Matsen, *Phys. Rev. Lett.* **80**, 4470 (1998).